Kalman Tracking and Bayesian Detection for Radar RFI Blanking

Weizhen Dong, Brian D. Jeffs
Department of Electrical and Computer Engineering
Brigham Young University
J. Richard Fisher
National Radio Astronomy Observatory, Green Bank
RFI 2004, Penticton, 17 July 2004

BYU
BRIGHAM YOUNG
UNIVERSITY

Introduction

- The Green Bank Telescope and other observatories experience significant L-band interference from air surveillance RADARs.
- This impulsive RFI is a prime candidate for time-domain, blanking-based mitigation.

- We present an improved blanking method which dynamically tracks moving aircraft echoes.
- The proposed algorithm was tested using real 1292 MHz RADAR data recorded by R. Fisher at the GBT.

.

RADAR Interference Geometry

- Transmitter is 104 km SSE of GBT.
- Weak line-of-sight signal.
- Strong local mountain terrain clutter.
- Multiple aircraft echoes are seen out to several hundred km.
- For aircraft tracking this is a “bi-static,” unco-operative RADAR scenario.

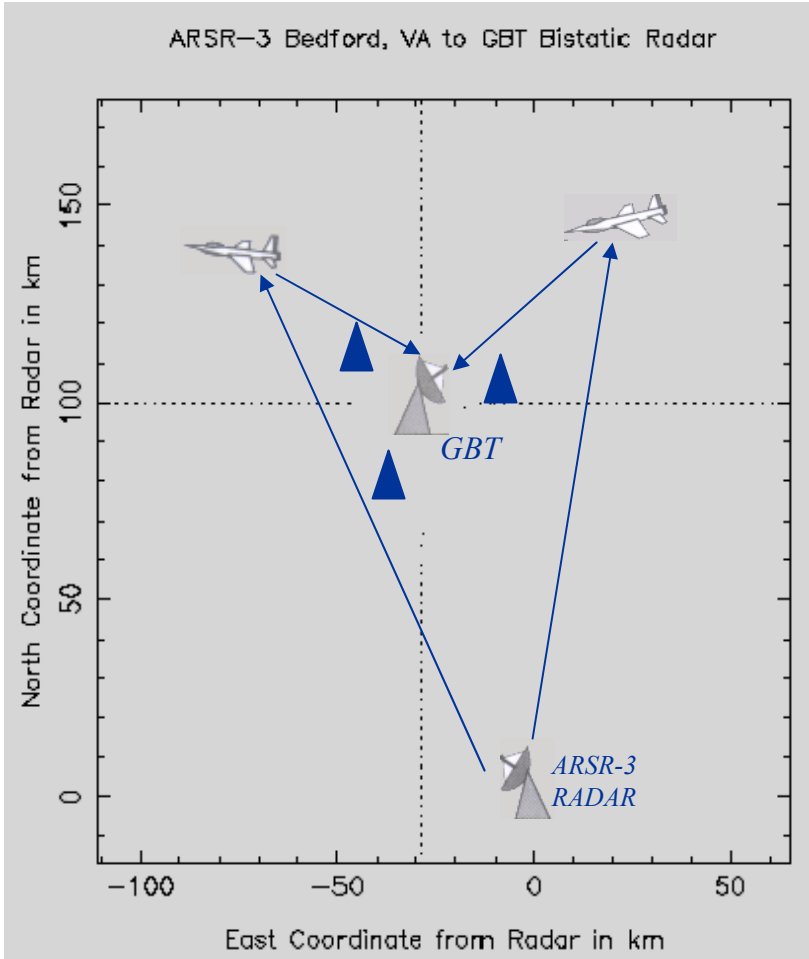

Baseline Solution

- Goal: Remove ARSR-3 Air Surveillance RADAR RFI from desired cosmic signal at the GBT.

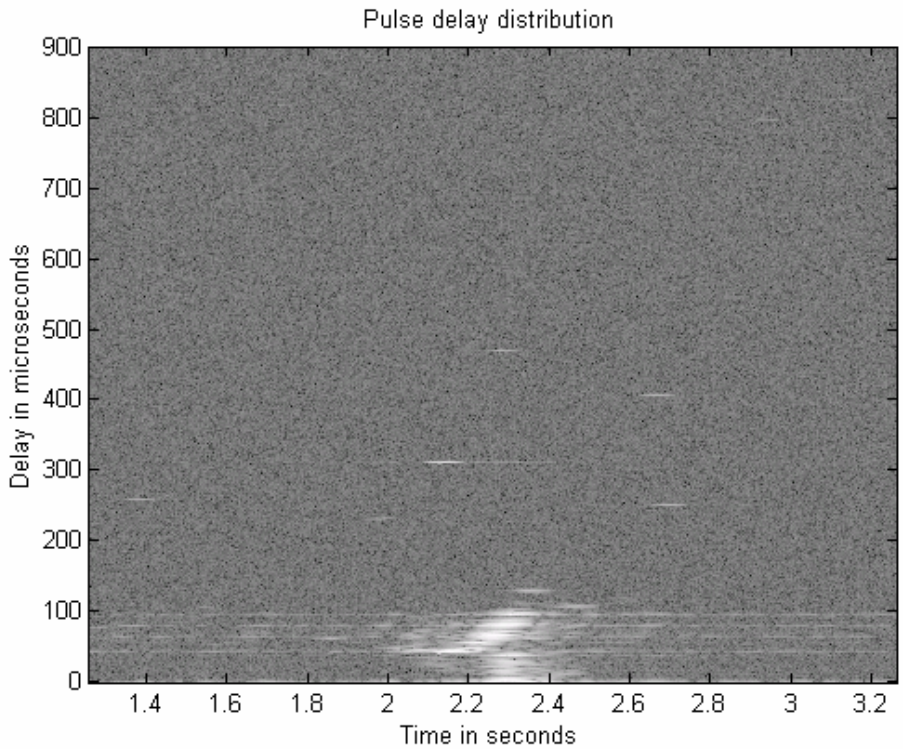

A 60° of a single antenna sweep overhead at GBT. Time series data is reordered into range-bearing bins

Baseline Solution

- Goal: Remove ARSR-3 Air Surveillance RADAR RFI from desired cosmic signal at the GBT.
- "Simple time window blanking" removes only fixed, repeatable local terrain clutter.

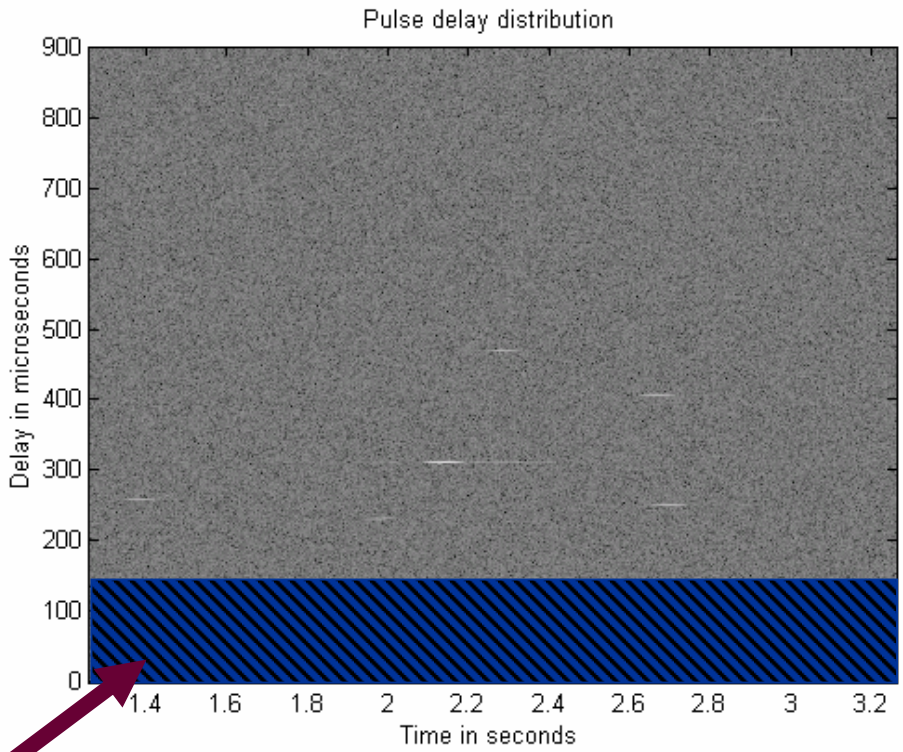

Zero out first 150 µs after first pulse arrival

A 60° of a single antenna sweep overhead at GBT. Time series data is reordered into range-bearing bins

Baseline Solution

- Goal: Remove ARSR-3 Air Surveillance RADAR RFI from desired cosmic signal at the GBT.
- "Simple time window blanking" removes only fixed, repeatable local terrain clutter.
- "Detected pulse blanking" suppresses many moveable aircraft echoes.

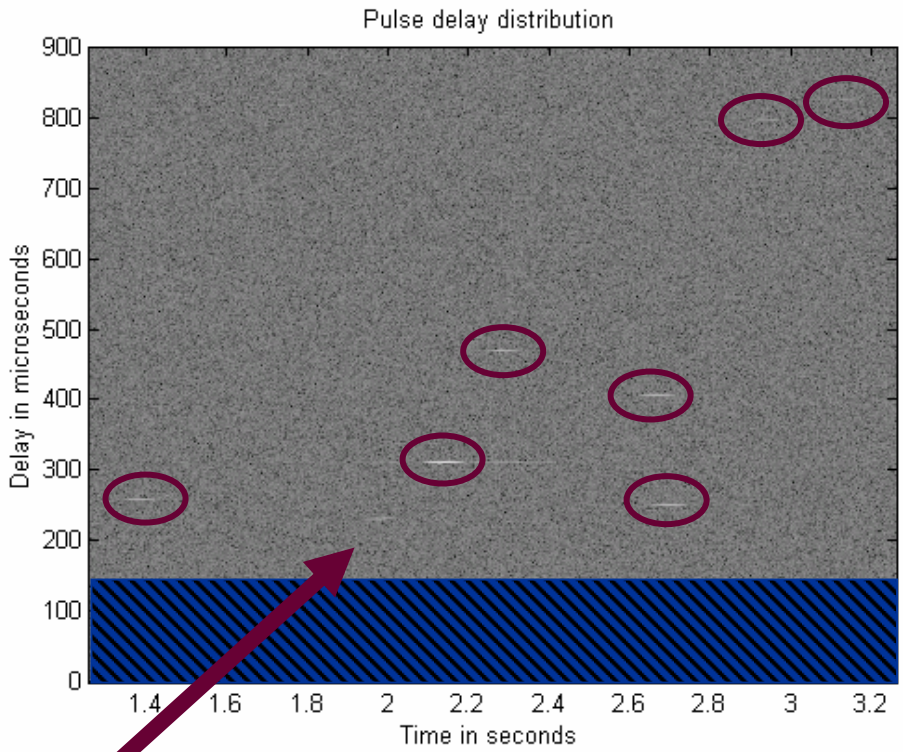

Weak echoes remain

A 60° of a single antenna sweep overhead at GBT. Time series data is reordered into range-bearing bins

Problem Statement

- Problems:
  - Cannot perform “detected pulse” aircraft blanking in *real-time* due to process delay.
  - With “detected pulse blanking,” weaker echoes are missed and can bias spectral estimates.
- Proposed approach:
  - Use a Kalman tracker to develop prior information on each aircraft.
    - Tracker predicts locations for next echo:
      1) Blank prediction region in real-time.
      2) Detector-blanker runs parallel with observation process.
    - Locally increase prior probability for echo pulse arrival in prediction region :

      Bayesian detector improves P_D for weak pulses.

Preliminaries: Digital Receiver

- Mix RF center frequency to complex baseband.

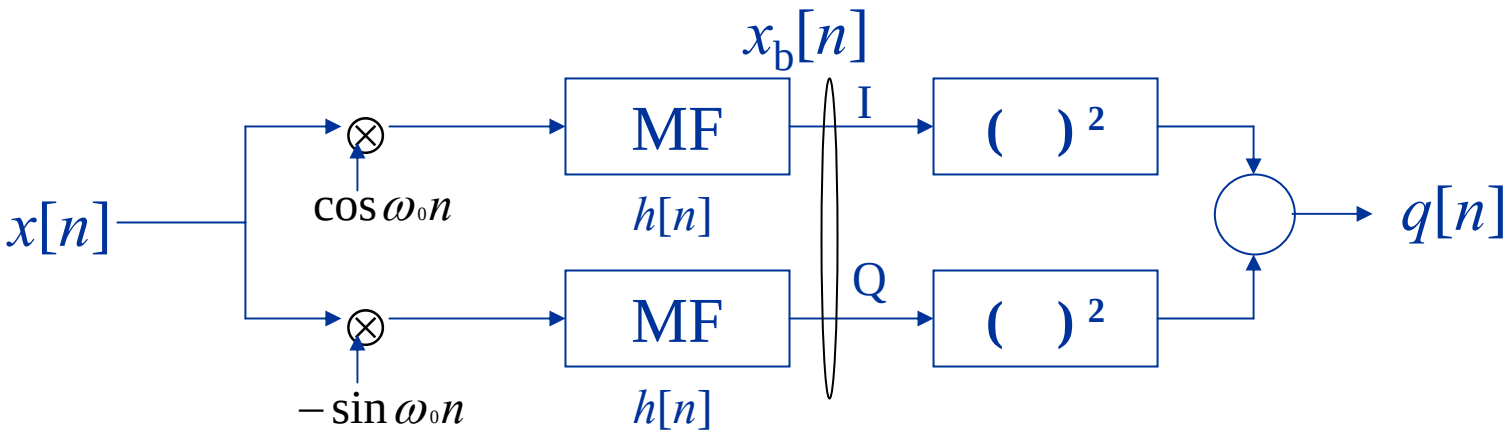

Where: $x[n]$ = sampled RF signal

$x_b[n]$ = complex baseband signal

q[n] = magnitude squared envelope for detection thresholding

ω_o = transmit pulse carrier frequency

$h[n]$ = matched filter impulse response

Preliminaries: Matched Filter Design

- Manual Hamming window fit to approximate to the transmitted pulse.

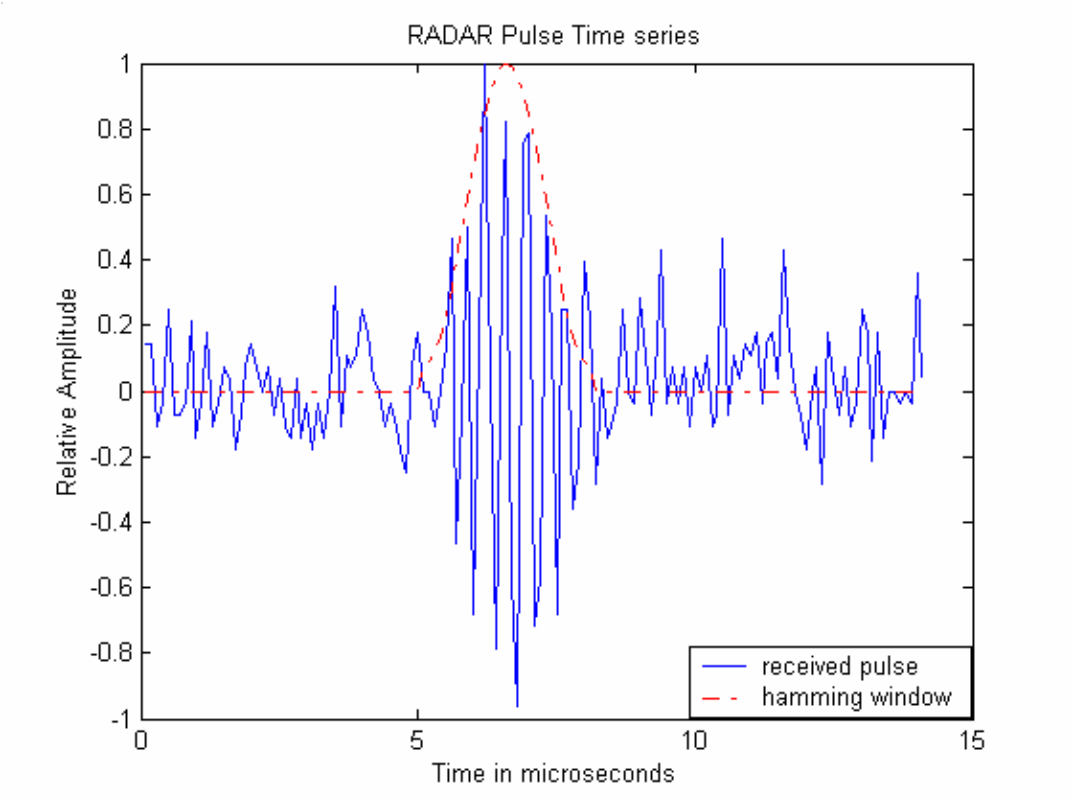

Preliminaries:
Modified CLEAN Algorithm

- Goal: Locate isolated echo points in overlapping ambiguity surfaces.
- Method: CLEAN iterative beampattern subtraction.
- Constraint: the process stops when residual peak is lower than detection threshold, τ_0.
  - Solve for the threshold, τ_0, by selecting a false alarm rate P_{FA}, such that

$$P_{FA} = \int_{\tau_0}^{\infty} f(q[n] \mid H_0) dq$$

  - $f(q[n]|H_0)$ is a Rayleigh distribution.

Preliminaries:
Modified CLEAN Algorithm (cont.)

- Examples of CLEAN detected echoes.
- Circles show two missed detection with conventional constant threshold algorithm.

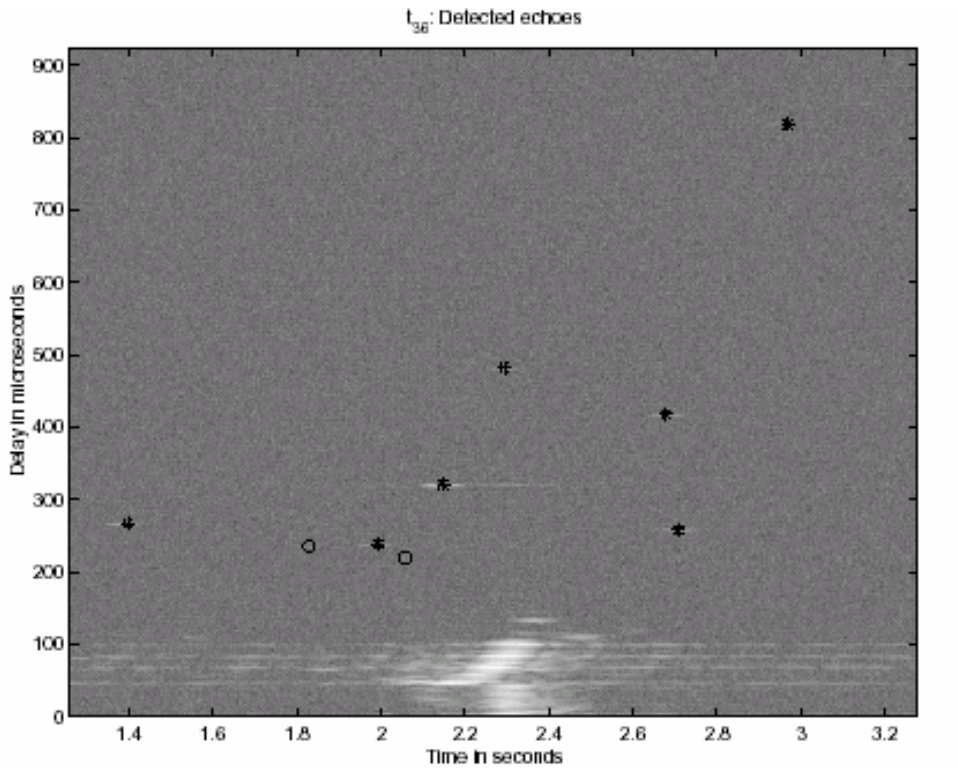

Kalman Tracker: State Equations

- Discrete-time, two-dimensional, two-state tracking.
- Sequentially estimate position & velocity of aircraft moving with constant velocity, perturbed by a zero mean random acceleration, $\boldsymbol{a}_n$.
- Snapshot sample interval is $T = t_{n+1} - t_n$.

$$\boldsymbol{x}_{n+1} = \boldsymbol{F}\boldsymbol{x}_n + \boldsymbol{G}\boldsymbol{a}_n, \quad \boldsymbol{x}_n = [x_n, y_n, \dot{x}_n, \dot{y}_n]^T,$$

$$\boldsymbol{F} = \begin{bmatrix} 1 & 0 & T & 0 \\ 0 & 1 & 0 & T \\ 0 & 0 & 1 & 0 \\ 0 & 0 & 0 & 1 \end{bmatrix}, \quad \boldsymbol{G} = \begin{bmatrix} \frac{T^2}{2} & 0 & T & 0 \\ 0 & \frac{T^2}{2} & 0 & T \end{bmatrix}^T$$

Kalman Tracker: Observation Equations

- Measurements, z_n, are noise corrupted in range and bearing by υ_n.
- Observations are polar, in range and bearing.
- Tracking is performed in the Cartesian coordinate system.

$$\boldsymbol{z}_n = \boldsymbol{h}(\boldsymbol{x}_n) + \boldsymbol{\upsilon}_n,$$

$$\boldsymbol{h}(\boldsymbol{x}_n) = \begin{bmatrix} \sqrt{x_n^2 + y_n^2} \\ \tan^{-1}\left(\frac{y_n}{x_n}\right) \end{bmatrix},$$

$$\boldsymbol{\upsilon}_n = \left[\upsilon_r(n), \upsilon_\theta(n)\right]^T$$

Kalman Tracker: Prediction and Update Equations

- This tracking system is nonlinear, so use an extended Kalman filter.

Prediction:

$$\hat{\boldsymbol{x}}(n+1\,|\,n) = \boldsymbol{F}\boldsymbol{x}(n\,|\,n),$$
$$\boldsymbol{P}(n+1\,|\,n) = \boldsymbol{F}\boldsymbol{P}(n|n)\boldsymbol{F} + \boldsymbol{G}\boldsymbol{Q}\boldsymbol{G},$$

Update:

$$\hat{\boldsymbol{x}}(n+1\,|\,n+1) = \hat{\boldsymbol{x}}(n+1\,|\,n) + \boldsymbol{K}(n+1)\left[\boldsymbol{z}(n+1) - \boldsymbol{h}(\hat{\boldsymbol{x}}(n+1\,|\,n)\right],$$
$$\boldsymbol{P}(n+1\,|\,n+1) = \left[\boldsymbol{I} - \boldsymbol{K}(n+1)\boldsymbol{H}(n+1)\right]\boldsymbol{P}(n+1),$$
$$\boldsymbol{K}(n+1) = \boldsymbol{P}(n+1\,|\,n)\boldsymbol{H}^T(n+1)\left[\boldsymbol{H}(n+1)\boldsymbol{P}(n+1\,|\,n)\boldsymbol{H}^T(n+1)\right]^{-1},$$
$$\text{where } \boldsymbol{H}(n+1) = \left[\frac{\partial \boldsymbol{h}}{\partial \boldsymbol{x}}\right]_{\boldsymbol{x}=\boldsymbol{x}(n+1|n)}$$

A Tracking Example with GBT Data

- 5 snapshots of CLEAN detections.
- Prediction points for snapshot n=6 shown.
- Prediction region ellipses have difference sizes depending on track quality.
- Size is proportional to prediction error variance in $\boldsymbol{P}(n+1|n)$.

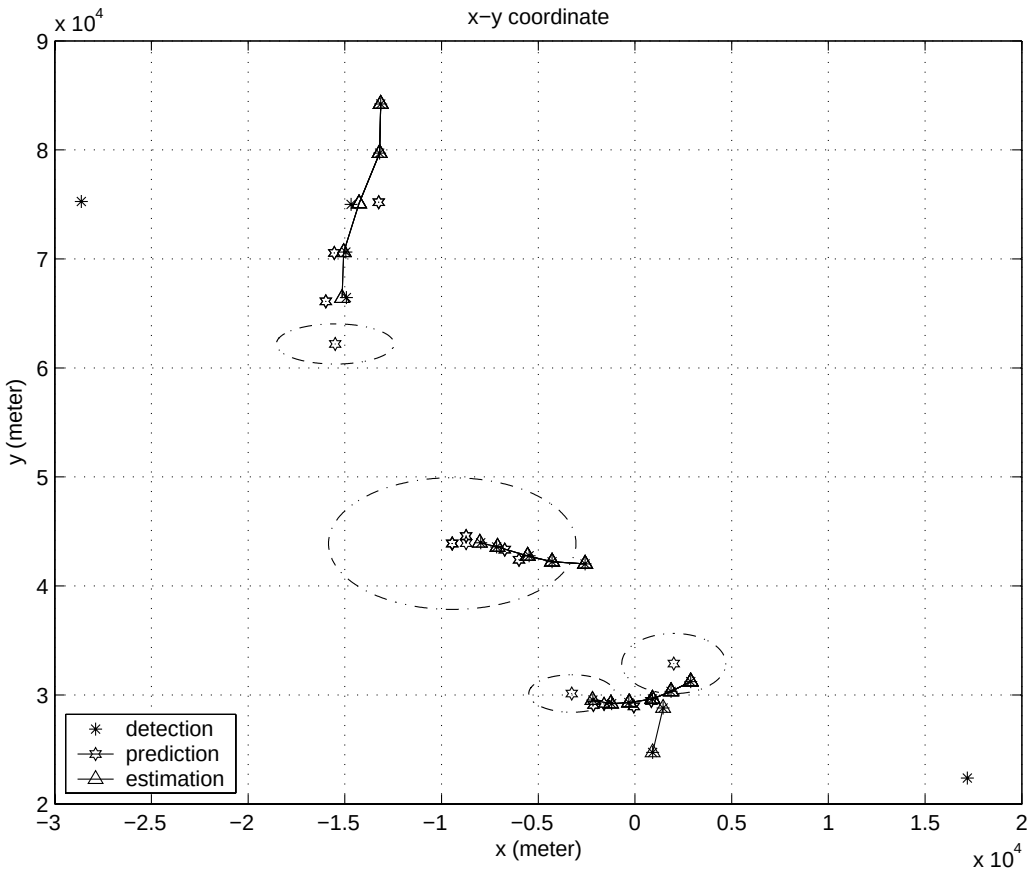

A Tracker-Based Prior Distribution for Bayesian Detection

- Pulse arrival prior distribution $f(x,y)$
  - Defined on elliptical prediction region:
    - Centroid: prediction point

      $(\hat{x}_{n+1|n}, \hat{y}_{n+1|n})$

    - Radii: proportional to

      $\sqrt{P_{n+1|n}(1,1)} \quad \sqrt{P_{n+1|n}(2,2)}$

  - Use a truncated elliptical Gaussian surface.

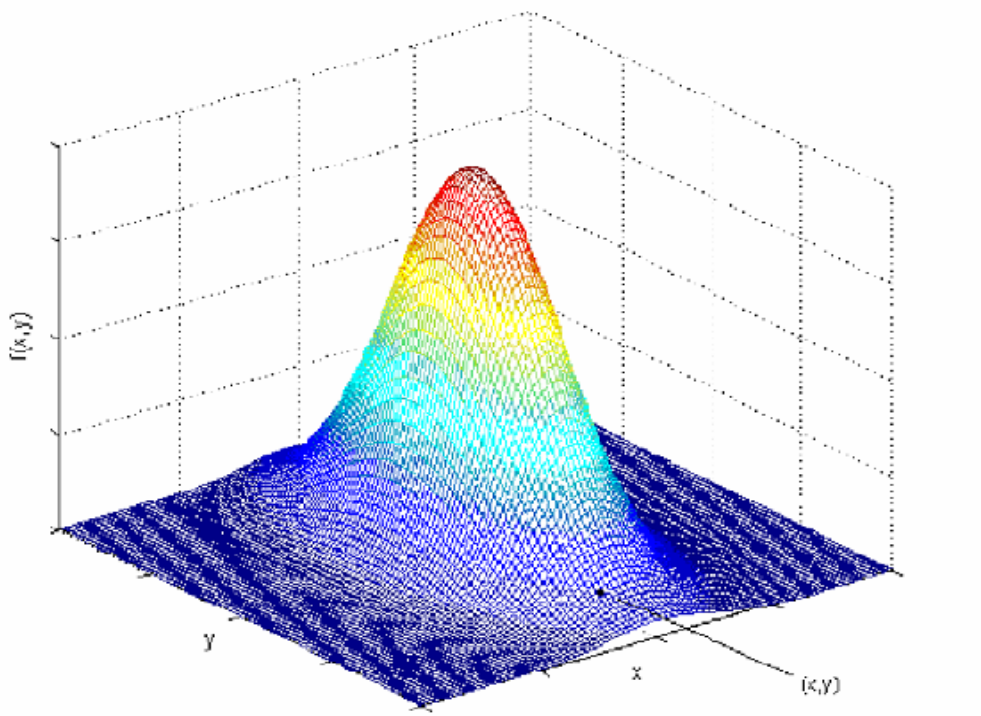

Probability of Presence of an Echo

- Integrating $f(x,y)$ over the corresponding polar patch yields probability of presence of an echo in a single range-bearing bin:

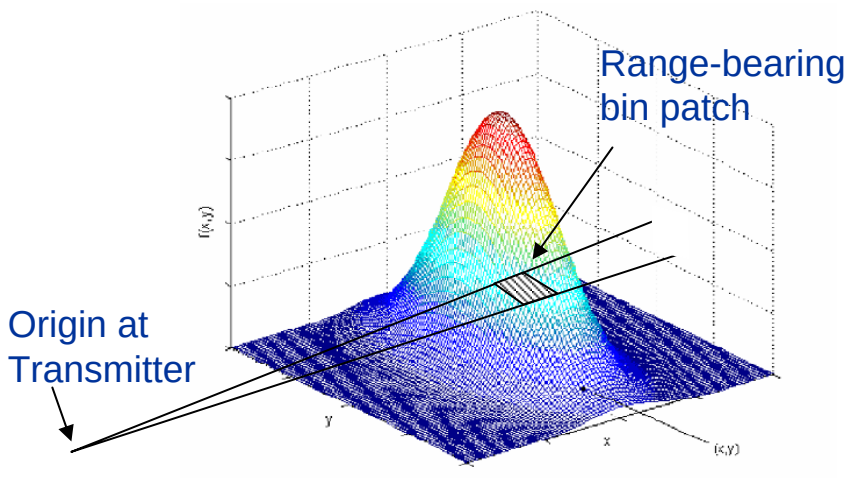

$$P(H_1) = Ce^{-\frac{r_{y1}^2}{2\sigma_y^2}},$$

$$P(H_0) = 1 - Ce^{-\frac{r_{y1}^2}{2\sigma_y^2}}$$

- Characteristics:
  - Probability decreases with distance from the prediction point.
  - Does not depend on gross range, R, but on ellipse axis length, r_{y1}, from bin to prediction point.

A Bayesian Constant False Alarm Rate Detector

- Define a new error metric: total probability of false alarm:

$$P_{TFA} = P(H_0)\, P_{FA}$$
$$= P(H_0) \int_{\tau}^{\infty} f(q[n] \mid H_0) dq.$$

  - This is the unconditional probability that a false alarm will occur at a given bin. P_{FA} is conditional on there being no echo present.
  - Uses prior information in track that an echo is likely.
- For constant total false alarm rate detection, solve for $\tau(x,y)$ at each range-bearing bin using $P(H_o)$ from track

$$P_{TFA} = P(H_0) \int_{\tau(x,y)}^{\infty} f(q[n] \mid H_0) dq = c, \text{ a constant.}$$

- Declare a detection by test:

$$\text{If } \; q[(n)|_{(x,y)}] > \tau(x,y), \; \text{decide } H_1.$$

Effect on Detection Threshold

- Results in decreased threshold for weaker pulses in regions with higher probability.
- $\tau(x,y)$ is position dependent, lower in prediction regions.

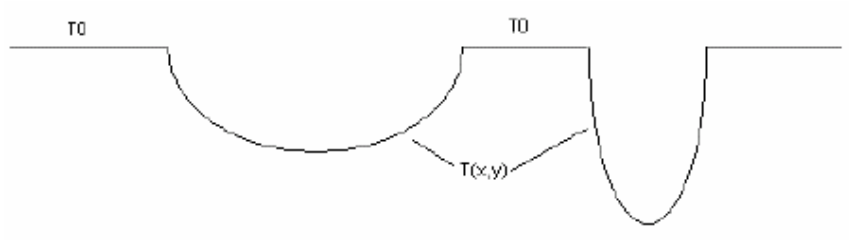

- Probability of detection is increased without significantly raising P_{FA}.
- Low quality tracks produce wider, less deep reduced threshold regions.

Simulated Experimental Results

- Sampled Receiver Operator Characteristic (ROC) curve comparison of the two algorithms.
- Monte-Carlo simulation for repeated random trials to evaluate P_D. v.s. P_{FA}.
- Bayesian method has uniformly higher P_D at all $P_{FA.}$

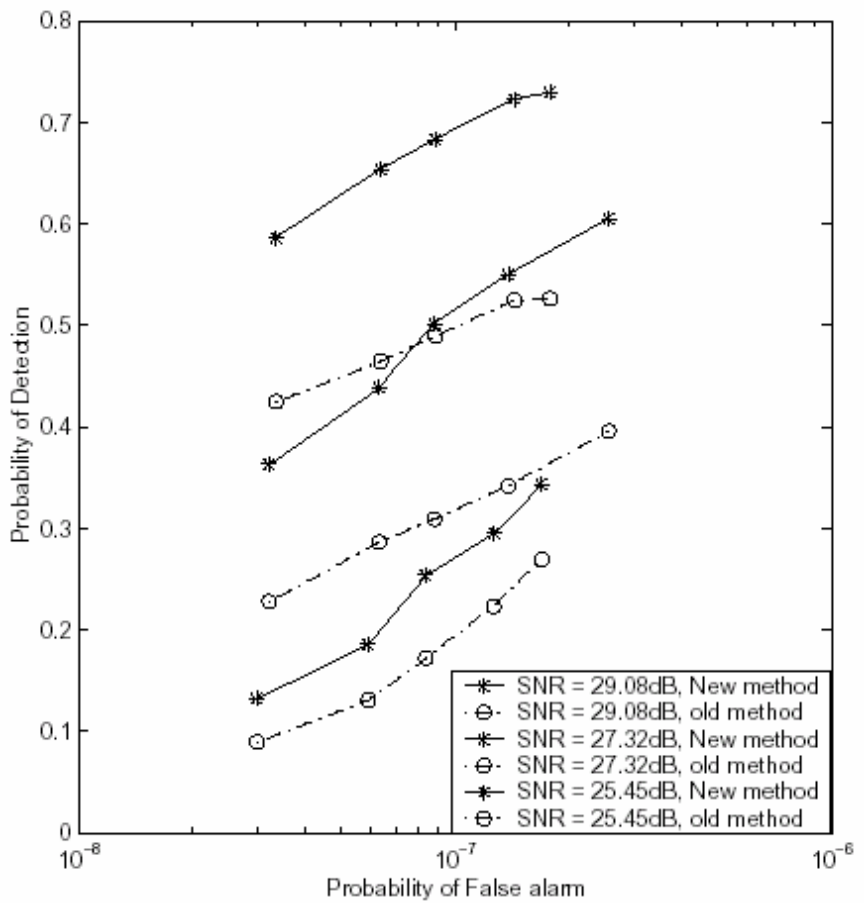

GBT Data Experimental Results

- Real data set 1 echo detection result:

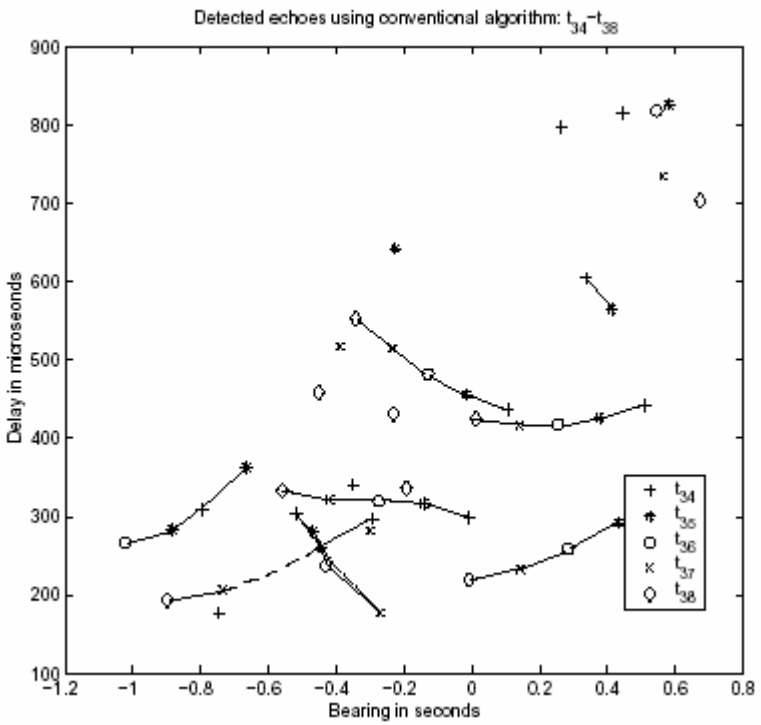

Conventional fixed P_{FA} detector

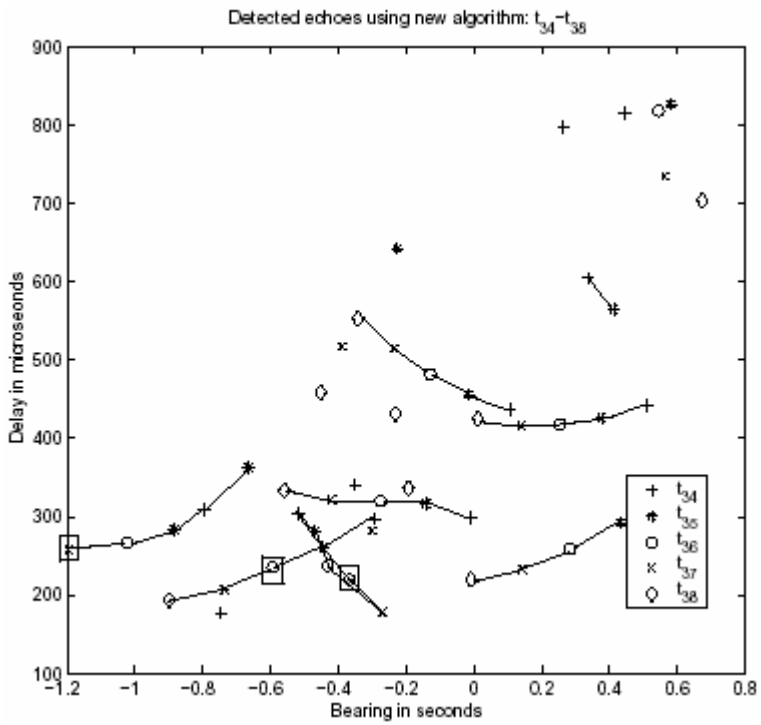

Bayesian fixed P_{TFA} detector

Note that 3 weak echoes (inside the rectangles) are detected by new algorithm.

Data Set 1 Blanking performance

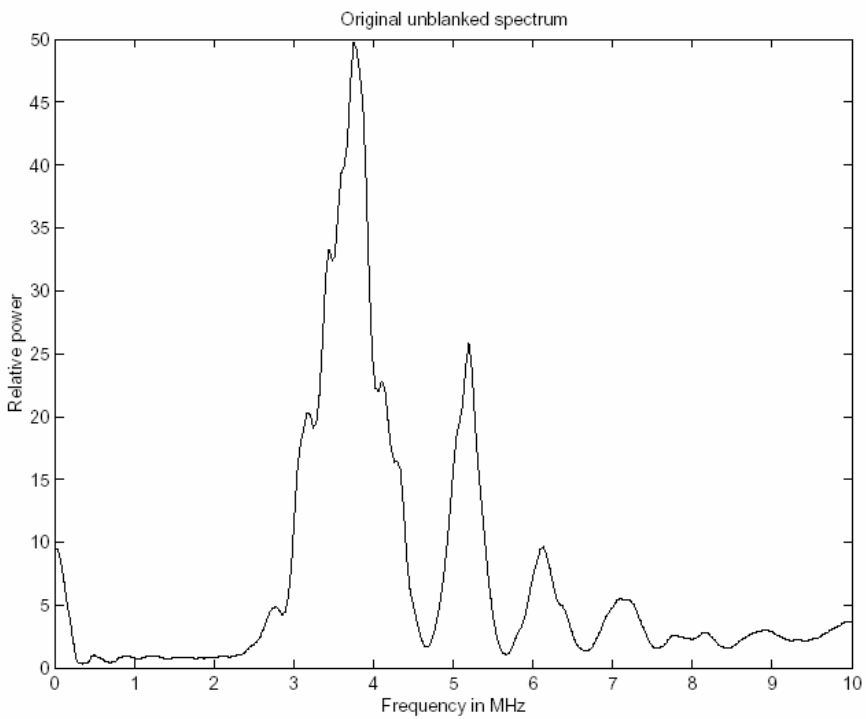

Unblanked spectrum.

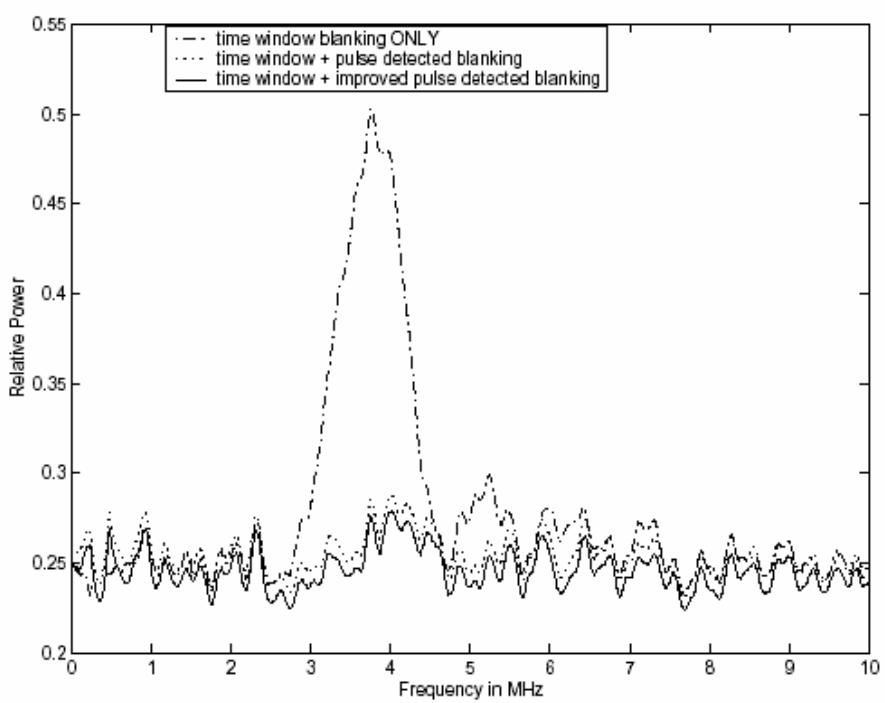

The spectra integrated: Top spectrum is for simple time window, which blanked 30 microseconds before and 150 microseconds after the earliest arriving pulses. Two bottom spectra are for window blanking combined with detected pulse blanking (conventional and new algorithms, respectively).

Real Data Set 2 Results, Matching P_{FA} between algorithms

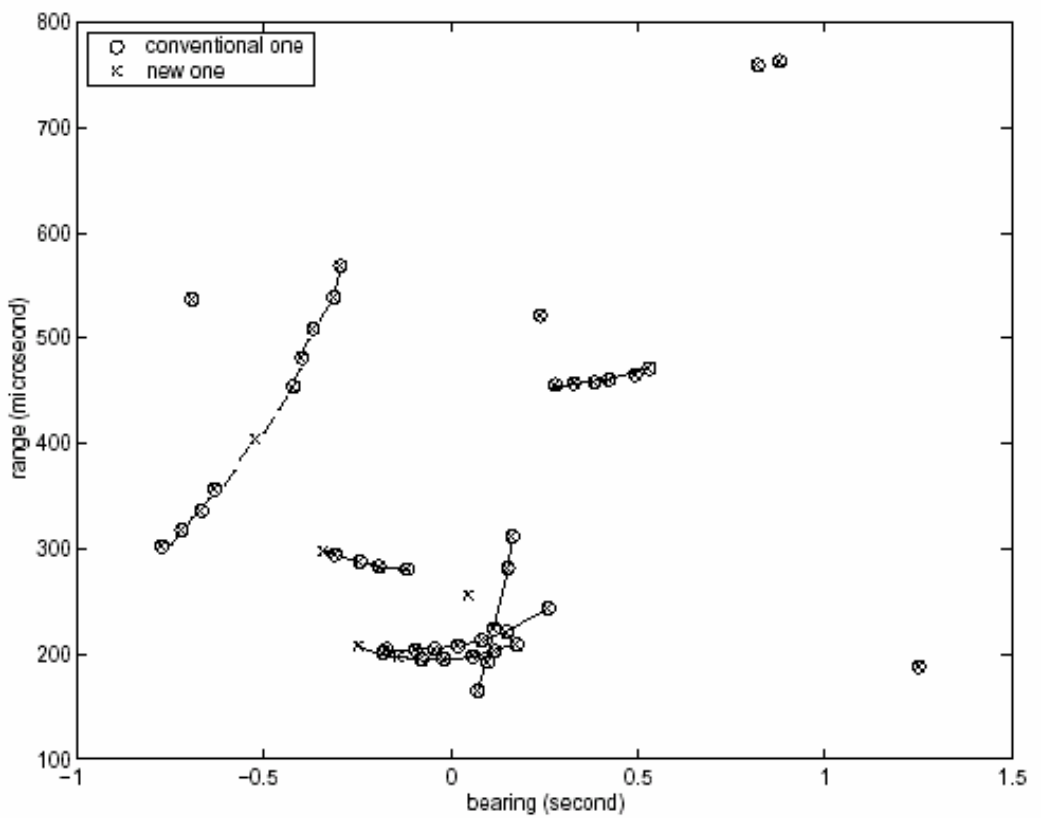

Detection tracks for both new and conventional algorithms.

$P_{FA} = 3.8676 \times 10^{-8}$.

The new algorithm detected some weaker echoes without additional false alarms.

Matching P_D between Algorithms

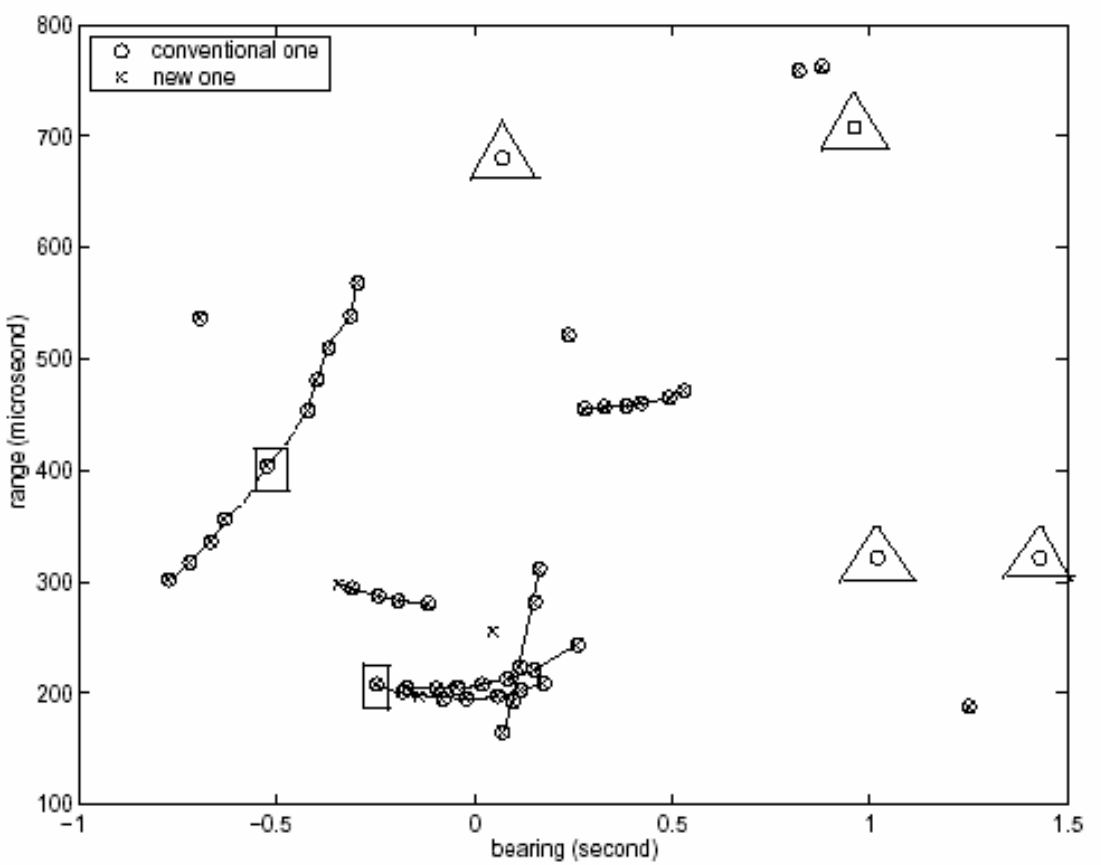

For the conventional algorithm we lowered the constant threshold to recover the two missed detections. $P_{FA} = 2.3205 \times 10^{-7}$.

This introduces four false alarms (inside triangles).

Data Set 2 Blanking Performance

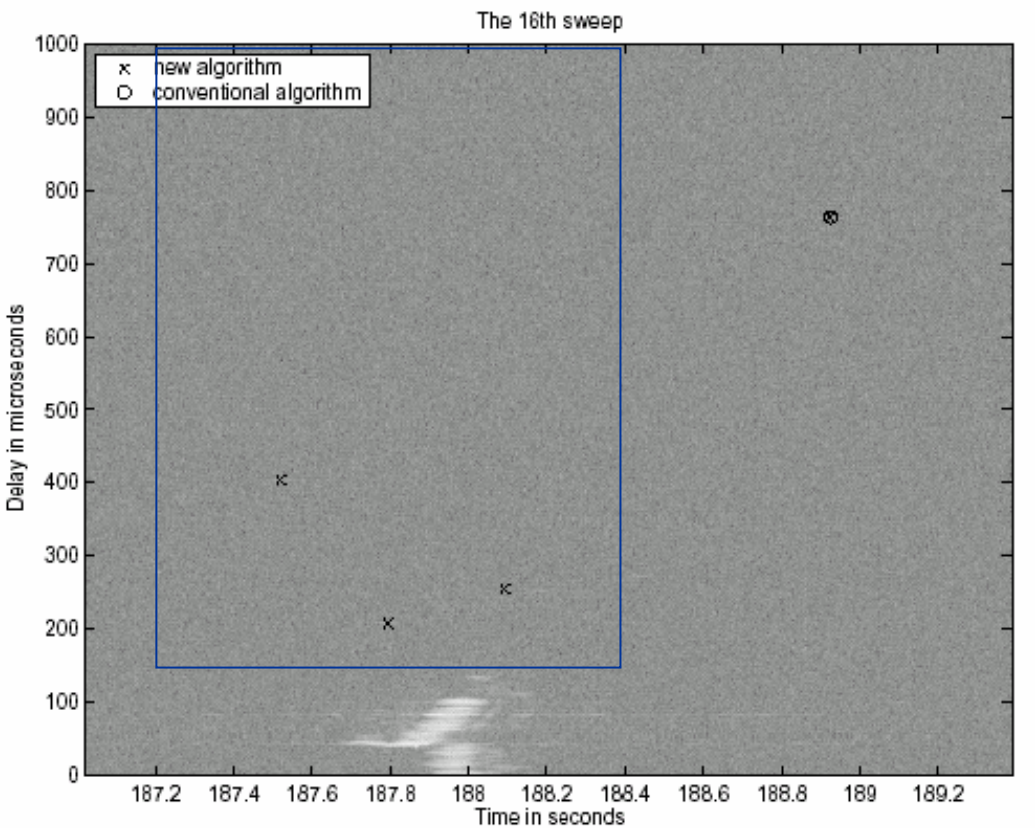

Spectrum was integrated from 187.2 to 188.4 seconds.

This includes three echoes missed by conventional fixed threshold detection.

Experimental Results (cont.)

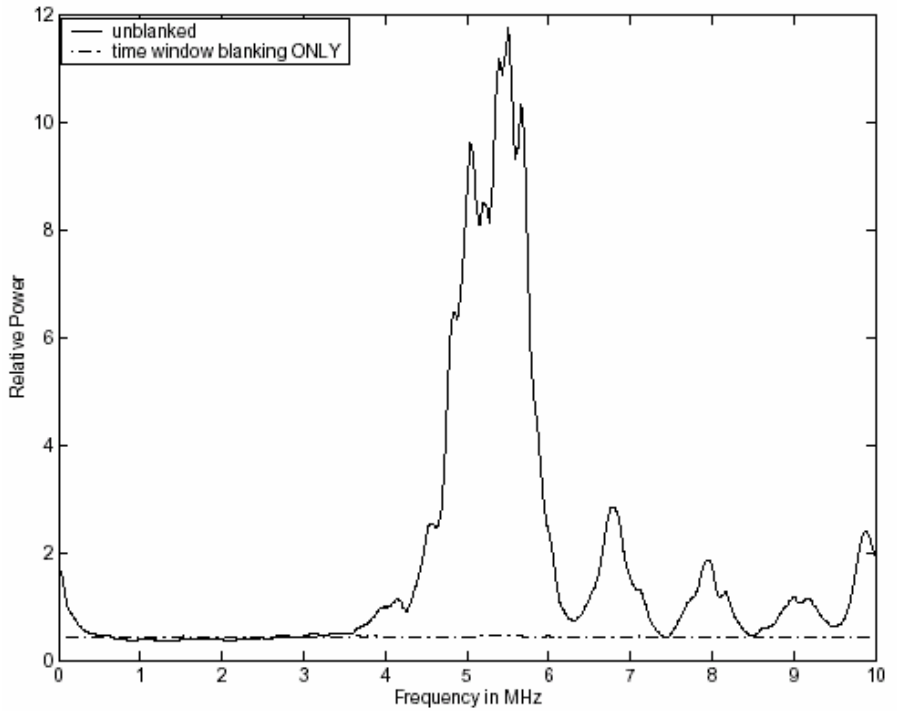

Unblanked v.s. simple time window blanked.

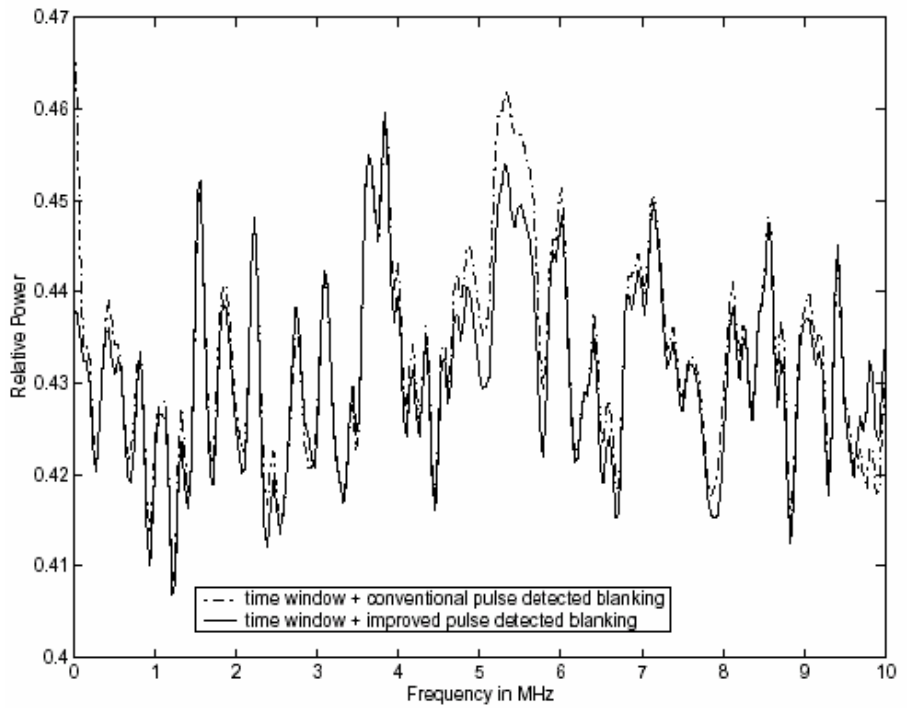

Time window blanking combined with detected pulse blanking (using new and conventional echo detection algorithms, respectively).

Conclusions

- Kalman tracking enables predictive real-time detected pulse blanking without a processing lag.
- A high speed DSP processor is required for real-time pulse detection.
- The Bayesian framework improves detection sensitivity, P_D, without increasing P_{FA}.
- Bayesian detection can be real time or post processing on recorded data.

Preliminaries: Pulse Time Alignment

- First arrival time of each pulse must be detected from the data to form range-bearing map.
  - Initial Alignment: approximate based on estimated global parameters:
    - Measured pulse repetition rate (PRF) = 341.4 Hz.
    - Periodic time offset of an integer multiples of 100 microseconds in sequence of [0,4,0,3,1,2,1,3].
  - Improved Alignment using CFAR detection

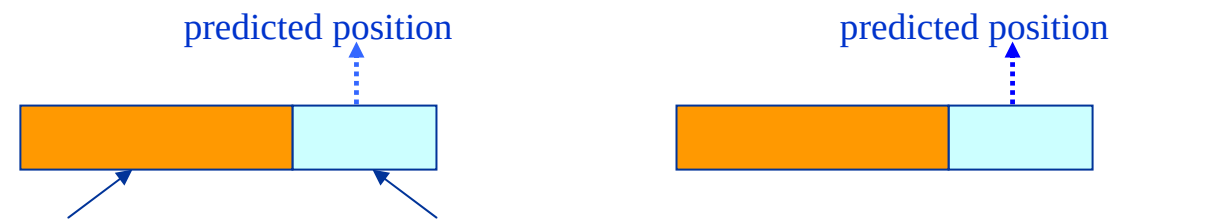

Preliminaries:
Pulse Time Alignment (cont.)

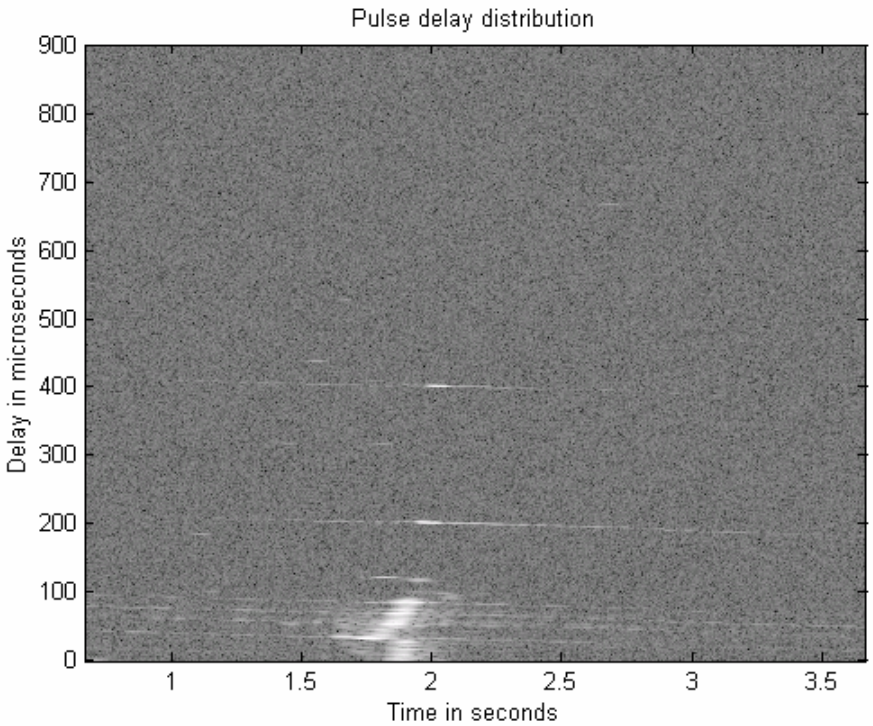

(a) Initial pulse time alignment

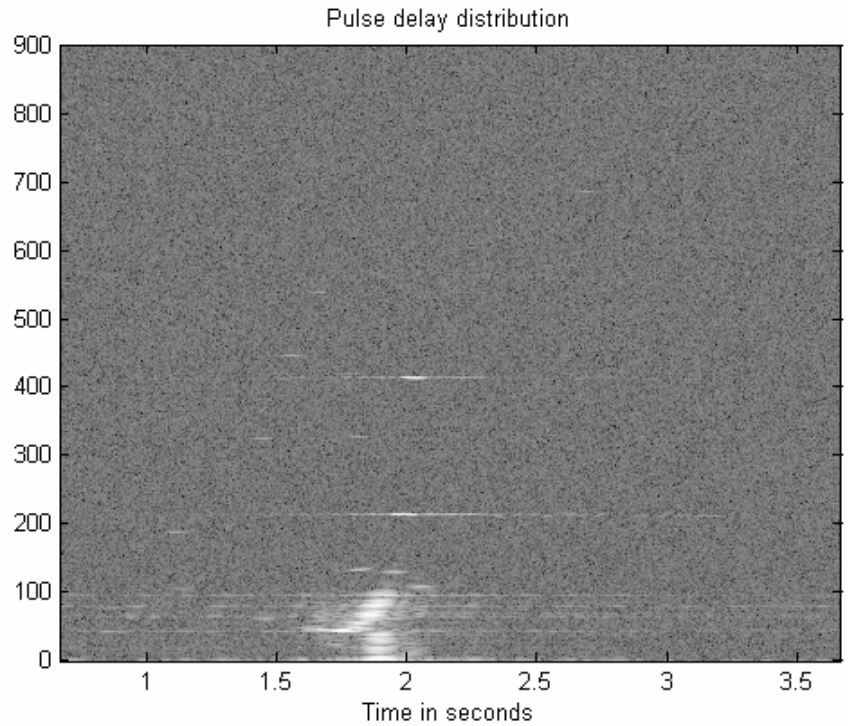

(b) Improved alignment using CFAR detection

Kalman Tracking (cont.)

- Track management tasks
  - Track Association
  - Missed detections
  - Dropping a track
  - Creating a new track
  - Splitting a track
- Two modes of operation:
  - Real-time processing: blanks the corrupted data before detection, using only prediction regions.
  - Post processing: blanks after detection. Exploit track history to improve detections